

Thermal voltage noise in layered superconductors

V. D. Ashkenazy

Department of Physics, Bar-Ilan University, 52100, Ramat Gan, Israel

G. Jung

*Department of Physics, Ben Gurion University of the Negev, 84105 Beer-Sheva, Israel
and Instytut Fizyki PAN, 02668 Warszawa, Poland*

B. Ya. Shapiro

*Jack and Pearl Resnick Institute of Advanced Technology, Bar-Ilan University, 52100, Ramat Gan, Israel
and Department of Physics, Bar-Ilan University, 52100, Ramat Gan, Israel*

(Received 3 October 1994)

Thermal voltage noise in the mixed state of type-II superconductors has been calculated taking into account fluctuation modes of nonrigid vortices. It has been shown that bending of vortices leads to new effects in thermal-voltage-noise spectra at high frequencies. The power spectrum reflecting fluctuations of rigid vortices is suppressed at very low frequencies and saturates into a white spectrum at a characteristic frequency depending on the strip width. At high frequencies tilt modes of flexible vortices start to contribute to the fluctuating voltages and the power spectrum undergoes three subsequent magnitude increases, following $\omega^{1/2}$ -, ω^2 -, and again $\omega^{1/2}$ -like behavior before becoming white again. It has been shown that for layered superconductors of a moderate anisotropy the second $\omega^{1/2}$ -like increase disappears at magnetic fields exceeding a certain threshold field corresponding to the crossover field between two-dimensional and three-dimensional vortex-lattice melting. Field dependencies of characteristic frequencies separating different regimes of spectral behavior have been evaluated and shown to be qualitatively different for low and high magnetic fields.

I. INTRODUCTION

Random motion of flux vortices in type-II superconductors leads to fluctuating voltages across the sample. It was shown by Li and Clem that voltage noise in a superconducting slab is determined by the motion of top and bottom edges of a vortex line, i.e., by the motion of the points at which the magnetic flux pierces sample surfaces.¹ Therefore, in the literature concerned with noise, vortices are usually regarded as rigid rods and degrees of freedom corresponding to their tilt are not taken into account; for a review see Ref. 2. At low frequencies, below a certain characteristic frequency, such an approximation is correct. In fact, the energy of a tilted vortex is proportional to the square of the wave vector corresponding to the tilt displacement. The shortest wave vectors are of the order of an inverse thickness of the sample. Usually, noise experiments are performed with samples in the form of thin strips. The small thickness of such samples sets the upper frequency limit of the applicability of the rigid-vortex approximation sufficiently high for a typical low-frequency noise experiment. Recently Hocquet, Mathieu, and Simon³ have considered tilts of vortex edges that result from interactions with surface roughness. Nevertheless, the internal part of a vortex line was still treated as a rigid rod.

The rigid-vortex approach evidently fails at high frequencies. In this paper we demonstrate that by taking into account all degrees of freedom of vortices, without

accounting for any surface effects, one obtains two additional, with respect to a rigid-vortex case, subsequent increases of the spectral density of voltage fluctuations. Spectral-density increases appear above characteristic frequencies. The first characteristic frequency is associated with long-wave tilt modes, as compared to the penetration depth, while the second one reflects the onset of thermal activation of short-wave tilt modes.

Evidently, flexibility of vortices is most likely to be observed in layered superconductors where topological excitations take the form of pointlike pancakes located in the layers. Interaction between pancakes results in the creation of flexible vortex stacks, weakly coupled as compared to three-dimensional (3D) vortices in continuous superconductors. Recently, such systems became a subject of intensive investigations, mostly due to the layered nature of anisotropic high- T_c superconducting oxides. The dynamics of the pancake lattice was considered by Bulaevskii *et al.* in a paper devoted to NMR in high- T_c superconductors.⁴ A characteristic feature of layered superconductors with a moderate anisotropy is the suppression of Josephson interlayer interactions at strong magnetic fields. Consequently, physical properties of these systems are significantly different at low and strong applied magnetic fields. Feigelman, Geshkenbein, and Larkin have considered 3D melting of the vortex lattice at low fields and 2D melting at strong fields.⁵ Glazman and Koshelev pointed out that thermal fluctuations of pancake vortices suppress the superconducting long-range

order along the c axis.⁶ Daemen *et al.* have demonstrated the existence of a decoupling phase transition line in the (H, T) plane above which the superconducting current along the c axis vanishes.⁷

In this paper we demonstrate that in a layered system with Josephson coupling between layers there is a crossover in the behavior of voltage-noise-power spectra at a characteristic threshold field. For low magnetic fields we predict three subsequent increases of voltage-noise spectra, following $\omega^{1/2}$ -, ω^2 -, and again $\omega^{1/2}$ -like dependencies. We show that the second $\omega^{1/2}$ -like increase of power-spectrum magnitude vanishes at magnetic fields exceeding the threshold field, which corresponds to the crossover field between 3D and 2D vortex-lattice melting. Moreover, we find that field dependencies of characteristic frequencies separating various regimes of spectral behavior are qualitatively different below and above the threshold field.

$$G[\varphi_n, \mathbf{A}] = \sum_n \int d^2R \left\{ \frac{d\epsilon_0}{2\pi} \left[\nabla_{n\parallel}^{(2)} \varphi_n + \frac{2\pi}{\phi_0} \mathbf{A}_{n\parallel}^{(2)} \right]^2 + E_J \left[1 - \cos \left[\varphi_{n+1} - \varphi_n + \frac{2\pi}{\phi_0} \int_{nd}^{(n+1)d} dz A_{\perp} \right] \right\} + \int d^3R \left[\frac{B^2}{8\pi} - \frac{\mathbf{B} \cdot \mathbf{H}}{4\pi} \right], \quad \epsilon_0 = \frac{\phi_0^2}{(4\pi\lambda_{\parallel})^2}, \quad E_J = \frac{\phi_0^2}{\pi(4\pi\lambda_{\perp})^2 d}. \quad (1)$$

The first term in the discrete sum describes the energy of superconducting condensate in the n th layer, $\nabla_{n\parallel}^{(2)}$ and $\mathbf{A}_{n\parallel}^{(2)}$ are two-dimensional vectors, while the second term in the sum accounts for Josephson coupling between the n th and $(n+1)$ th layers. We use the symbols \parallel and \perp to denote parallel and perpendicular orientation with respect to the layer plane. In order to find the distribution of fields and currents in a layered superconductor, instead of a single equation appropriate for a continuous superconductor, one should solve the following set of London equations:

$$\frac{1}{\lambda_{\parallel}^2} \left[\frac{\phi_0}{2\pi} \nabla_{n\parallel}^{(2)} \varphi_n - \mathbf{A}_{n\parallel}^{(2)} \right] + (\Delta_{\parallel} + \Delta_{\perp}) \mathbf{A}_{n\parallel}^{(2)} = 0, \quad (2a)$$

$$\frac{1}{\lambda_{\perp}^2} \left[\frac{\phi_0}{2\pi} \nabla_{\perp} \varphi_n - \mathbf{A}_{\perp n} \right] + (\Delta_{\parallel} + \Delta_{\perp}) \mathbf{A}_{\perp n} = 0, \quad (2b)$$

$$\nabla_{\parallel}^{(2)} \mathbf{A}_{n\parallel}^{(2)} + \nabla_{\perp} \mathbf{A}_{\perp n-1} = 0, \quad (2c)$$

where symbols ∇_{\perp} and Δ_{\perp} denote the lattice gradient and the lattice Laplace operator, defined as $\nabla_{\perp} f_n \equiv (f_{n+1} - f_n)/d$, and

$$\Delta_{\perp} f_n \equiv (f_{n+1} + f_{n-1} - 2f_n)/d^2.$$

Since in layered superconductors Abrikosov vortices consist of chains of pancakes located in superconducting planes, therefore the equilibrium distribution of fields and currents at which the Gibbs potential (1) reaches the minimum is given by the solution of the system (2a)–(2c) completed by the following topological relation:

II. BASIC EQUATIONS

A. Vortices in layered superconductors

The criterion usually adopted to define a crossover between a continuous anisotropic and a discrete layered superconducting system is the smallness of the coherence length along the direction perpendicular to the layers, ξ_{\perp} , with respect to the separation between the layers, d . The basis for a phenomenological description of layered superconductors was formulated by Lawrence and Doniach.⁸ They treated the Gibbs functional in the London approximation, assuming that a constant modulus of order parameter describes a discrete set of superconducting layers located in the x - y plane, separated by a distance d along the z direction, and coupled together by a Josephson coupling term depending only on the phase difference of the order parameter, $\varphi_{n+1} - \varphi_n$, in the layers

$$\text{curl}_{\parallel} \nabla_{\parallel}^{(2)} \varphi_n = 2\pi \mathbf{e}_z \sum_{\mathbf{r}_n} \delta(\mathbf{r}_{\parallel} - \mathbf{r}_n). \quad (3)$$

Here, \mathbf{r}_n are the coordinates of pancakes in the n th layer and \mathbf{e}_z is the unit vector in the z direction. The Gibbs functional (1) is the function of radius vectors \mathbf{r}_n according to Eqs. (2a)–(2c) and (3).

In this paper we consider an ideal superconducting strip containing an Abrikosov lattice of pancake vortex chains induced by an external magnetic field applied perpendicular to the strip surface and layer plane. The strip possesses length L in the x direction, width W in the y direction, and thickness D in the z direction, such that $L \gg W \gg D$. The superconducting layers are lying in x - y plane and are separated by a distance d . Voltage measuring leads are attached to the strip at points with coordinates $[0,0]$ and $[L,0]$; see Fig. 1. We assume that the strip is carrying no transport current and that the temperature is kept constant. Pancake vortices are free to undergo thermally activated movements out of their

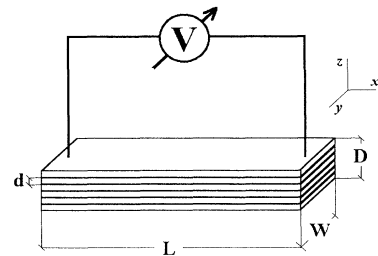


FIG. 1. The geometry of the problem.

equilibrium positions. We limit our discussion to low temperatures, in the sense that we do not allow for the melting of the vortex lattice. Therefore we assume that the displacements of pancakes from their equilibrium positions are small and it is allowed to use a harmonic approximation for the elastic energy of the vortex system.

Positions of pancakes in the film are described by three-dimensional vectors \mathbf{r}_p . For a pancake with an equilibrium position \mathbf{a}_{p0} in the Abrikosov lattice frame (ALF) we write

$$\mathbf{r}_p = \mathbf{a}_{p0} + \mathbf{u}(\mathbf{a}_{p0}, t), \quad (4)$$

where $\mathbf{u}(\mathbf{a}_{p0}, t)$ is a 2D vector in the layer plane. The energy of interaction between pancakes can be written in the harmonic approximation:

$$U[\mathbf{u}(\mathbf{a}_{p0}, t)] = \frac{1}{2} \sum_{ps} \hat{D}(p, s) \mathbf{u}(\mathbf{a}_{p0}, t) \mathbf{u}(\mathbf{a}_{s0}, t), \quad (5)$$

where $\hat{D}(p, s)$ is a 2D elastic matrix depending only on the vector $\mathbf{a} \equiv \mathbf{a}_{p0} - \mathbf{a}_{s0}$, i.e., we have $\hat{D}(p, s) \equiv \hat{D}(\mathbf{a})$. Vortex deviations $\mathbf{u}(\mathbf{a}_{p0}, t)$ can be expanded in the basis of polarization vectors $\boldsymbol{\varepsilon}(\mathbf{q}, \nu)$ diagonalizing the dynamic matrix $\hat{D}(\mathbf{q})$:

$$\hat{D}(\mathbf{q}) = \sum_{\mathbf{a}} \hat{D}(\mathbf{a}) \exp(i\mathbf{q}\mathbf{a}), \quad (6)$$

$$\hat{D}(\mathbf{q}) \boldsymbol{\varepsilon}(\mathbf{q}, \nu) = D_{\mathbf{q}\nu} \boldsymbol{\varepsilon}(\mathbf{q}, \nu), \quad (7)$$

$$\mathbf{u}(\mathbf{a}_{p0}, t) = \sum_{\mathbf{q}\nu} \boldsymbol{\varepsilon}(\mathbf{q}, \nu) \exp(i\mathbf{q}\mathbf{a}_{p0}) Q_{\mathbf{q}\nu}, \quad (8)$$

$Q_{\mathbf{q}\nu}(t)$ are normal-mode amplitudes, and \mathbf{q} and ν are the wave vector and polarization, respectively. Since $\mathbf{u}(\mathbf{a}_{p0}, t)$ lies in the layer plane there are two polarizations defined by the relative orientation of vectors $\boldsymbol{\varepsilon}(\mathbf{q}, \nu)$ and \mathbf{q}_{\parallel} . As will be shown below, for striplike geometries only modes with longitudinal polarization are meaningful in calculating voltages due to vortex motion. Elastic constants associated with these modes can be conveniently expressed in terms of the dispersive elastic moduli⁶

$$D_{\mathbf{q}l0} = \left[\frac{\phi_0 d}{B} \right] [C_{11} q_{\parallel}^2 + C_{44} \bar{q}_{\perp}^2], \quad \bar{q}_{\perp} \equiv \frac{2}{d} \sin(q_{\perp} d / 2). \quad (9)$$

The bulk compressive modulus C_{11} corresponds to longitudinal displacements of vortex lines. For a dense Abrikosov lattice, $H_{c1} \ll H \ll H_{c2}$ and $\lambda_{\parallel} \ll \lambda_{\perp}$, C_{11} is given by the well-known equation^{6,9,10}

$$C_{11} = \frac{B^2 [1 + \lambda_{\perp}^2 (q_{\parallel}^2 + \bar{q}_{\perp}^2)]}{4\pi [1 + \lambda_{\parallel}^2 (q_{\parallel}^2 + \bar{q}_{\perp}^2)] [1 + \lambda_{\perp}^2 q_{\parallel}^2 + \lambda_{\parallel}^2 \bar{q}_{\perp}^2]}. \quad (10)$$

For the tilt modulus C_{44} we adapt the form given by^{6,10}

$$C_{44} = \frac{B^2}{4\pi} \frac{1}{1 + q_{\parallel}^2 \lambda_{\perp}^2 + \bar{q}_{\perp}^2 \lambda_{\parallel}^2} + \frac{\phi_0 B \chi}{2(4\pi \lambda_{\perp})^2} + \frac{\phi_0 B}{2\bar{q}_{\perp}^2 (4\pi \lambda_{\parallel}^2)^2} \ln(1 + \bar{q}_{\perp}^2 / K_0^2), \quad (11)$$

$$\chi = \ln \left[\frac{k_{\max}^2}{K_0^2 + (\bar{q}_{\perp} \lambda_{\parallel} / \lambda_{\perp})^2} \right], \quad K_0 = (4\pi B / \phi_0)^{1/2},$$

$$k_{\max} \sim 1 / \xi_{\parallel} (1 + T / T_1)^{-1/2}, \quad T_1 \sim \frac{2\phi_0^2 \varepsilon_{\parallel}^2}{(4\pi)^2 \lambda_{\perp}^2 d}, \quad (12)$$

where ξ_{\parallel} is the coherence length in the layer plane.

Observe that the equation for C_{44} consists of three terms. The first term corresponds to a nonlocal contribution to the tilt energy; the second and third terms are caused by deformations of separate vortex lines. The second term, the Josephson coupling term, can be neglected at strong magnetic fields. However, for the strongly anisotropic case, $\lambda_{\perp} d \gg \lambda_{\parallel}^2$, it can be neglected for all magnetic fields. In the following we shall consider a case of moderate anisotropy $\xi_{\perp} \ll d \ll \lambda_{\parallel}^2 / \lambda_{\perp}$, at which Josephson coupling cannot be *a priori* neglected.

B. Voltage noise due to vortex motion

Following Li and Clem,¹ we write for the voltage produced by a flux line moving within a flat slab of a uniform thickness

$$V_i = \mathbf{g}(\boldsymbol{\rho}_{ip}^i) \frac{\partial \boldsymbol{\rho}_{ip}^i}{\partial t} - \mathbf{g}(\boldsymbol{\rho}_{bt}^i) \frac{\partial \boldsymbol{\rho}_{bt}^i}{\partial t}, \quad (13)$$

where $\boldsymbol{\rho}_{ip}^i$ and $\boldsymbol{\rho}_{bt}^i$ denote 2D coordinates of pancakes belonging to i th flux line in the top and in the bottom layer of the film, respectively. For a continuous superconductor $\boldsymbol{\rho}_{ip}^i$ and $\boldsymbol{\rho}_{bt}^i$ are simply associated with the top and bottom coordinates of the vortex. The resolution factor $\mathbf{g}(\boldsymbol{\rho})$ is determined by the geometry of the measuring circuit:

$$\mathbf{g}(\boldsymbol{\rho}) = \frac{\phi_0}{4\pi I_m} [\mathbf{b}_{mtp}(\boldsymbol{\rho}) - \mathbf{b}_{mbt}(\boldsymbol{\rho})], \quad (14)$$

where \mathbf{b}_{mtp} and \mathbf{b}_{mbt} are the values of magnetic induction due to the current flow I_m in the measuring circuit on the top and on the bottom of a slab, respectively.

The resolution function $\mathbf{g}(\boldsymbol{\rho})$ for a strip arrangement, such as that shown in Fig. 1, takes the form^{2,11}

$$\mathbf{g}(\boldsymbol{\rho}_{ip;bt}^i) = \pm \frac{\phi_0}{2cW} \mathbf{e}_y. \quad (15)$$

Assuming that the difference $\boldsymbol{\rho}_{ip}^i - \boldsymbol{\rho}_{bt}^i$ is much smaller than the characteristic length at which the resolution function $\mathbf{g}(\boldsymbol{\rho})$ changes, i.e., much smaller than the strip width W , we have simply $\mathbf{g}(\boldsymbol{\rho}_{ip}^i) = -\mathbf{g}(\boldsymbol{\rho}_{bt}^i) = \mathbf{g}(\boldsymbol{\rho}_i)$. Now, we can express the total voltage due to vortex movement in terms of vortex current density $\mathbf{J}(\boldsymbol{\rho}, t)$:

$$V(t) = \int d^2 \boldsymbol{\rho} \mathbf{g}(\boldsymbol{\rho}) \mathbf{J}(\boldsymbol{\rho}, t), \quad (16)$$

where the integral (16) is taken over the entire specimen, and

$$\mathbf{J}(\boldsymbol{\rho}, t) = \mathbf{J}_{ip}(\boldsymbol{\rho}, t) + \mathbf{J}_{bt}(\boldsymbol{\rho}, t),$$

$$\mathbf{J}_{ip;bt}(\boldsymbol{\rho}, t) = \sum_i \mathbf{v}_{ip;bt}^i(t) \delta_2[\boldsymbol{\rho} - \boldsymbol{\rho}_{ip;bt}^i(t)], \quad (17)$$

$$\mathbf{v}_{ip;bt}^i = \frac{d\boldsymbol{\rho}_{ip;bt}^i}{dt}.$$

The fluctuating component of the voltage (16) can be expressed in terms of fluctuations of the vortex current density $\delta\mathbf{J}(\rho, t) = \mathbf{J}(\rho, t) - \langle \mathbf{J}(\rho, t) \rangle$, where $\langle \cdots \rangle$ stands for the time average:

$$\delta V(t) = V(t) - \langle V(t) \rangle_t = \int d^2\rho \mathbf{g}(\rho) \delta\mathbf{J}(\rho, t). \quad (18)$$

Consequently, the voltage autocorrelation function

$$\begin{aligned} \Psi_V(\tau) &= \langle \delta V(t) \delta V(t + \tau) \rangle \\ &= \int d^2\rho \int d^2\rho' \sum_{\alpha\beta} g_\alpha(\rho) g_\beta(\rho') \mathbf{K}_{\alpha\beta}(\rho, \rho', \tau) \end{aligned} \quad (19)$$

will be expressed in terms of the vortex-flow correlation function

$$K_{\alpha\beta}(\rho, \rho', \tau) = \langle \delta\mathbf{J}_\alpha(\rho, t) \delta\mathbf{J}_\beta(\rho', t + \tau) \rangle, \quad (20)$$

where α and β are Cartesian coordinates. If the dimen-

sions of the measuring circuit are large with respect to the intervortex spacing the vortex lattice can be treated as a continuum. Since we have assumed small displacements of vortices from their equilibrium positions, within the first-order approximation, the change in the vortex-flow density is

$$\begin{aligned} \delta\mathbf{J}(\rho, t) &= n_0 [\delta\mathbf{v}_{tp}(\rho - \mathbf{v}_0 t, t) + \delta\mathbf{v}_{bt}(\rho - \mathbf{v}_0 t, t)] \\ &\quad + \mathbf{v}_0 [\delta n_{tp}(\rho - \mathbf{v}_0 t, t) + \delta n_{bt}(\rho - \mathbf{v}_0 t, t)], \end{aligned} \quad (21)$$

where n_0 is the equilibrium vortex-line density, $\delta\mathbf{J}$ and ρ are vectors in the laboratory reference frame, and $\delta\mathbf{v}$ and δn are measured in the ALF system moving with a velocity \mathbf{v}_0 . We identify $\delta\mathbf{v}_{tp;bt}$ as $d\mathbf{u}_{tp;bt}/dt$ and $\delta n_{tp;bt}$ as $[-n_0 \nabla \mathbf{u}_{tp;bt}]$, where $d\mathbf{u}_{tp;bt}$ is the displacement of a pancake on the top/bottom of the strip. In terms of normal modes in the ALF,

$$\delta\mathbf{J}(\rho, t) = n_0 \sum_{\mathbf{q}_{\parallel\nu}} \exp[i\mathbf{q}_{\parallel}(\rho - \mathbf{v}_0 t)] \sum_{\mathbf{q}_\perp} \cos\left[\frac{q_\perp D}{2}\right] \left[\boldsymbol{\varepsilon}(\mathbf{q}_{\parallel\nu}) \frac{dQ_{\mathbf{q}\nu}}{dt} - i\mathbf{v}_0 \mathbf{q}_{\parallel} \cdot \boldsymbol{\varepsilon}(\mathbf{q}_{\parallel\nu}) Q_{\mathbf{q}\nu}(t) \right]. \quad (22)$$

Putting $\delta\mathbf{J}$ from Eq. (22) into Eq. (18) we obtain for the voltage fluctuation

$$\delta V(t) = \sum_{\mathbf{q}_{\parallel\nu}} \delta V_{\mathbf{q}_{\parallel\nu}}(t), \quad (23)$$

$$\begin{aligned} \delta V_{\mathbf{q}_{\parallel\nu}}(t) &= \sum_{\mathbf{q}_\perp} \cos\left[\frac{q_\perp D}{2}\right] \left[P_{\mathbf{q}_{\parallel\nu}} \frac{dQ_{\mathbf{q}\nu}(t)}{dt} + G_{\mathbf{q}_{\parallel\nu}} Q_{\mathbf{q}\nu}(t) \right] \\ &\quad \times \exp(-i\mathbf{q}_{\parallel} \mathbf{v}_0 t), \end{aligned} \quad (24)$$

where

$$P_{\mathbf{q}_{\parallel\nu}} = n_0 \int d^2\rho \mathbf{g}(\rho) \cdot \boldsymbol{\varepsilon}(\mathbf{q}_{\parallel\nu}) \exp(i\mathbf{q}_{\parallel}\rho), \quad (25)$$

and

$$G_{\mathbf{q}_{\parallel\nu}} = -n_0 \int d^2\rho \mathbf{g}(\rho) \cdot \mathbf{v}_0 \exp(i\mathbf{q}_{\parallel}\rho) [i\mathbf{q}_{\parallel} \cdot \boldsymbol{\varepsilon}(\mathbf{q}_{\parallel\nu})]. \quad (26)$$

Observe that there are two contributions to the voltage noise in Eq. (24). The first one is proportional to velocity fluctuations, i.e., to $dQ_{\mathbf{q}\nu}/dt$, while the second term is proportional to vortex density fluctuations, i.e., to $Q_{\mathbf{q}\nu}$. For the considered long strip case, factors $P_{\mathbf{q}_{\parallel\nu}}$ and $G_{\mathbf{q}_{\parallel\nu}}$ can be calculated using Eq. (15):

$$P_{\mathbf{q}\nu} = \frac{|\mathbf{B}|L}{c} \frac{\sin(\mathbf{q}_\perp W/2)}{\mathbf{q}_\perp W} \delta_{\mathbf{q}_\perp, 0} \delta_{\nu, lo}, \quad (27)$$

$$G_{\mathbf{q}\nu} = \mathbf{q} \cdot \mathbf{v}_0 P_{\mathbf{q}\nu}, \quad (28)$$

where $\delta_{a,b}$ is the Kronecker symbol.

The phenomenological equation of a force balance for the moving p th pancake is

$$\eta_p \frac{d\mathbf{r}_p}{dt} = - \sum_s \hat{D}(p, s) \mathbf{u}(s, t) + \mathbf{F}_{\text{ext}}(\mathbf{r}_p, t), \quad (29)$$

where η_p is the viscosity of a single pancake, connected

to the commonly used vortex viscosity per unit length η by a simple relation $\eta = \eta_p/d$.¹² The external force $\mathbf{F}_{\text{ext}}(\rho_p, t)$ is acting in the layer plane, while the vortex-vortex interaction term is accounted for according to Eq. (5). Taking the time average of the force balance equation (29) we obtain for displacements of vortices from their equilibrium positions

$$\eta_p \frac{d\mathbf{u}(\mathbf{a}_{p0}, t)}{dt} + \sum_s G(p, s) \mathbf{u}(\mathbf{a}_{s0}, t) = \delta\mathbf{F}(\mathbf{a}_{p0}, t), \quad (30)$$

where $\delta\mathbf{F} = \mathbf{F}_{\text{ext}} - \langle \mathbf{F} \rangle$. Expanding Eq. (30) by the normal displacements, we obtain

$$\eta_p \frac{dQ_{\mathbf{q}\nu}(t)}{dt} + D_{\mathbf{q}\nu} Q_{\mathbf{q}\nu}(t) = \delta F_{\mathbf{q}\nu}(t), \quad (31)$$

where

$$\delta F_{\mathbf{q}\nu} = \frac{1}{N} \sum_s \exp(-i\mathbf{q}\mathbf{a}_{s0}) \boldsymbol{\varepsilon}(\mathbf{q}\nu) \delta\mathbf{F}(\mathbf{a}_{s0}, t), \quad (32)$$

and N is the number of pancakes in the sample. The solution of Eq. (31) is

$$Q_{\mathbf{q}\nu} = \int_{-\infty}^{\infty} \frac{d\omega}{2\pi} \sigma_\nu(\mathbf{q}, \omega) \delta F_{\mathbf{q}\nu}(\omega) \exp(-i\omega t), \quad (33)$$

$$\sigma_\nu(\mathbf{q}, \omega) = [D_{\mathbf{q}\nu} - i\omega\eta_p]^{-1}. \quad (34)$$

The knowledge of the fluctuating component of the external force, $\delta\mathbf{F}$, enables us to calculate $Q_{\mathbf{q}\nu}$, $dQ_{\mathbf{q}\nu}/dt$, and thus the resulting noise voltage. In the considered case, the Abrikosov lattice is stationary and $v_0 = 0$. The driving force for vortices is the Langevin force which it is uncorrelated in direction, space, and time, and has a zero time average:

$$\begin{aligned} \langle F_\alpha(\mathbf{a}_{p0}, t) F_{\alpha'}(\mathbf{a}_{s0}, t') \rangle &= T\eta_p \delta_{\alpha\alpha'} \delta_{ps} \delta(t-t'), \\ \langle \mathbf{F}(t) \rangle &= 0, \end{aligned} \quad (35)$$

where T stands for the temperature measured in energy units. The voltage autocorrelation function is then

$$\Psi_v(\tau) = \sum_{\mathbf{q}_\parallel \mathbf{q}'_\parallel} P_{\mathbf{q}_\parallel} (P_{\mathbf{q}'_\parallel})^* \sum_{\mathbf{q}_\perp \mathbf{q}'_\perp} \left\langle \frac{dQ_{\mathbf{q}_\perp}(t)}{dt} \frac{dQ_{\mathbf{q}'_\perp}^*(t+\tau)}{dt} \right\rangle. \quad (36)$$

By using Eqs. (33) and (35) this can be shown to be

$$\begin{aligned} \Psi_v(\tau) &= \frac{T\eta_p}{2\pi N} \sum_{\mathbf{q}_\parallel} |P_{\mathbf{q}_\parallel}|^2 \sum_{\mathbf{q}_\perp} \cos^2 \left[\frac{\mathbf{q}_\perp D}{2} \right] \\ &\quad \times \int_{-\infty}^{\infty} \frac{\omega^2 \exp(-i\omega\tau)}{D_{\mathbf{q}_\perp}^2 + \eta_p^2 \omega^2} d\omega. \end{aligned} \quad (37)$$

The power spectrum follows directly as

$$S_v(\omega) = \frac{T\eta_p}{N} \sum_{\mathbf{q}_\parallel} |P_{\mathbf{q}_\parallel}|^2 \sum_{\mathbf{q}_\perp} \cos^2 \left[\frac{\mathbf{q}_\perp D}{2} \right] \frac{\omega^2}{D_{\mathbf{q}_\perp}^2 + \eta_p^2 \omega^2}. \quad (38)$$

Since the factor $P_{\mathbf{q}_\parallel}$ is proportional to the Kronecker symbol $\delta_{\mathbf{q}_x,0}$ one can replace summation over \mathbf{q}_\parallel by summation over $\mathbf{q}_{\parallel y}$. For simplicity of notation the index y in $\mathbf{q}_{\parallel y}$ will be omitted in the rest of the paper.

III. SPECTRAL DENSITY OF VOLTAGE NOISE

The fluctuating behavior of a layered superconductor depends on the frequency range and on the applied magnetic field. For sufficiently low frequencies, even in layered systems, chains of pancake vortices form stacks that tge behave like rigid-vortex lines. Above the crossover, frequency tilt modes can be excited and fluctuations corresponding to bending of vortices dominate the spectral properties of the resulting voltage noise. The qualitative behavior of fluctuating tilted pancake stacks depends on the applied magnetic field. At low fields the Josephson coupling between the layers plays a significant role and the system behaves as a 3D one. At high magnetic fields, above the crossover field, the layered superconductor behaves as a 2D system.⁵

A. Transition between rigid and flexible behavior of fluctuating pancake strings

At low frequencies, below the characteristic crossover frequency determined by the strip thickness, the behavior of strings of pancakes is identical to that of rigid vortices. The minimal nonzero values of \mathbf{q}_\perp are of the order of $1/D \gg 1/W$; therefore, since $C_{11} \leq C_{44}$ for all $\mathbf{q}_\perp \neq 0$, we have $C_{11} \mathbf{q}_\perp^2 \ll C_{44} \mathbf{q}_\perp^2$. Consequently, at frequencies much smaller than the characteristic frequency

$$\omega_D = \frac{\phi_0 B}{4\pi\eta D^2}, \quad (39)$$

terms with $\mathbf{q}_\perp = 0$ prevail and Eq. (38) yields for the power spectrum

$$S_v(\omega) = \frac{T\eta_p}{N} \sum_{\mathbf{q}_\parallel} |P_{\mathbf{q}_\parallel}|^2 \frac{\omega^2}{C_{11}^2 \mathbf{q}_\parallel^4 + \eta_p^2 \omega^2}, \quad \omega \ll \omega_D. \quad (40)$$

Passing from summation to integration in Eq. (40) we find that for extremely small frequencies, much smaller than the characteristic frequency ω_W which depends on the strip width,

$$\omega_W = \frac{\phi_0 B}{4\pi\eta W^2}, \quad (41)$$

the power spectrum is increasing with increasing frequency as

$$S_v(\omega) = \frac{\phi_0 B L T}{2\pi c^2 W \eta D} \left[\frac{\omega}{2\omega_W} \right]^{1/2}, \quad \omega \ll \omega_W. \quad (42)$$

In the range $\omega_W \ll \omega \ll \omega_D$ one immediately gets the white spectrum of magnitude

$$S_v(\omega) = S_{v1} = \frac{\phi_0 B L T d}{\pi c^2 W \eta_p D} \int_0^\infty \frac{\sin^2 x}{x^2} dx = \frac{\phi_0 B L T}{2c^2 W \eta D}. \quad (43)$$

Qualitatively, this picture corresponds to the thermal-noise spectra considered by Li and Clem for an infinite film containing rigid vortices.¹ However, the functional dependence obtained by Li and Clem at low frequencies differs from the one predicted by Eq. (42). The $\sqrt{\omega}$ functional dependence was recently obtained by us for rigid vortices in the strip geometry.¹³

For frequencies larger than the crossover frequency ω_D all terms in the summation over \mathbf{q}_\perp in Eq. (38) are significant and the first term in the expression for the elastic constants, Eq. (9), is negligible. Spectrum (38) becomes determined by the properties of the elastic modulus C_{44} . As was mentioned above, the main contribution to voltage fluctuations is given by long-wave fluctuations in the layer planes, i.e., by the fluctuations that are changing at distances of the order of the characteristic size of the measuring circuit. In our case such a characteristic length is set by the width of the strip W . Formally, it means that due to the fact that the factor $|P_{\mathbf{q}_\parallel}|^2$ is proportional to the function $(\mathbf{q}_y W)^{-2} \sin^2(\mathbf{q}_y W/2)$ [see Eq. (27)] the dominating contribution in the sum over \mathbf{q}_\parallel in Eq. (38) is given by terms with $\mathbf{q}_\parallel \leq W^{-1}$. It follows from the natural condition $\lambda_1 \ll W$ that in our problem we are entitled to neglect the elastic moduli dependence on \mathbf{q}_\parallel and thus, consequently, neglect the third term in Eq. (11).

Since at high frequencies all summation terms in spectrum (38) have to be taken into account, we pass to the integration over \mathbf{q}_\perp , replace the quickly oscillating factor $\cos^2(\mathbf{q}_\perp D/2)$ by its average value 0.5, and obtain for the power spectrum at frequencies above the crossover ω_D

$$S_v(\omega) = \frac{\phi_0 B L T \eta_p d}{8\pi c^2 W} \int_{-\pi/d}^{\pi/d} \frac{\omega^2 d \mathbf{q}_\perp}{[(\phi_0 d/B) C_{44}]^2 \mathbf{q}_\perp^4 + \eta_p^2 \omega^2}. \quad (44)$$

The integral (44) cannot be calculated analytically in the general case. However, one can obtain analytical asymptotical solutions for different limiting frequency ranges. Before proceeding in this direction, let us observe that strong dependence of the tilt modulus C_{44} on magnetic field results in strong dependence of the power spectra on magnetic field. Careful examination of Eq. (11) leads to the conclusion that there exists a threshold magnetic field B_{th} above which for all q_{\perp} the first term in Eq. (11) becomes significantly larger than the second one. The threshold field determined from this condition is of the order of

$$B_{th} \sim \frac{\phi_0 \lambda_{\parallel}^2}{(4\pi \lambda_{\perp})^2 d^2}. \quad (45)$$

Note that the threshold field thus determined corresponds to the well-known crossover field between 2D and 3D vortex-lattice melting.⁵

B. Fluctuations of flexible pancake strings: Low magnetic fields

At low applied magnetic fields the magnetic interaction between pancakes in the same layer is comparable to the Josephson interaction between pancakes in the adjacent layers. Therefore long-wave fluctuations are determined by the magnetic nonlocal term of the tilt elastic modulus, while the Josephson term corresponds to short-wave fluctuations. Spectrum (44) possesses several intrinsic characteristic frequencies. The highest one corresponds to the frequency at which modes with wave vectors $q_{\perp} \sim 1/d$ are excited:

$$\omega_d = \frac{\phi_0 \chi}{16 \lambda_{\perp}^2 d^2 \eta}. \quad (46)$$

Thus for frequencies from the range $\omega_D \ll \omega \ll \omega_d$ the dominating contribution to the spectrum (42) is provided by small wave vectors $q_{\perp} \ll 1/d$. Within this frequency range we are entitled to replace \bar{q}_{\perp} by q_{\perp} and to extend the integration limits to $\pm\infty$. The logarithmic dependence of quantity χ on q_{\perp} in Eq. (12) is very slow. We neglect the logarithmic dependence and put $q_{\perp} \sim a_0/\lambda_{\perp} \lambda_{\parallel}$. As a result, in the first order of the small quantity $(a_0/\lambda_{\perp})^2$, where $a_0 = (\phi_0/B)^{1/2}$, we obtain

$$S_v(\omega) = \frac{\phi_0 B T L}{16 W c^2 \eta \lambda_{\parallel}} \left[\frac{\beta - \beta^3}{\beta^2 \cos(\varphi/2)} + \frac{\beta^3 (\omega/\omega_{\lambda})^{1/2}}{\alpha^{1/2} \cos(\varphi/2 - \pi/4)} \right], \quad (47)$$

$$\beta = \left[\frac{\omega^2}{\omega_{\lambda}^2 + \omega^2} \right]^{1/4},$$

$$\varphi = \arcsin \left[\frac{\omega_{\lambda}^2}{\omega_{\lambda}^2 + \omega^2} \right]^{1/2}, \quad \alpha = \frac{a_0^2 \chi}{4\pi \lambda_{\perp}^2},$$

where the new characteristic frequency is defined as follows:

$$\omega_{\lambda} = \frac{\phi_0 B}{4\pi \eta \lambda_{\parallel}^2}. \quad (48)$$

For frequencies from the range $\omega_D \ll \omega \ll \omega_{\lambda}$ the power spectrum is given by

$$S_v(\omega) = \frac{\phi_0 B T L}{8 W c^2 \eta \lambda_{\parallel}} \left[\left[\frac{\omega}{2\omega_{\lambda}} \right]^{1/2} + \left[\frac{\omega}{\omega_{\lambda}} \right]^2 (4\alpha)^{-1/2} \right]. \quad (49)$$

There are two frequency-dependent terms in Eq. (49). The contribution of both terms becomes equal at frequencies of the order of

$$\omega_c \sim \frac{\phi_0^{4/3}}{\eta (4\pi)^{4/3} \lambda_{\parallel}^2 \lambda_{\perp}^{2/3}} B^{2/3} \quad (50)$$

and the functional dependence of the spectrum changes from $\omega^{1/2}$ to ω^2 . In the lower frequency subrange, $\omega_D \ll \omega \ll \omega_c$, the power spectrum is dominated by long-wave tilt modes with $q_{\perp} \leq (4\pi \eta \omega / \phi_0 B)^{1/2} \ll 1/\lambda_{\parallel}$. The elastic energy corresponding to such displacements is proportional to the dispersionless nonlocal modulus $C_{44} \approx B^2/4\pi$. Within the upper frequency subrange with ω^2 dependence, $\omega_c \leq \omega \leq \omega_{\lambda}$, modes with $q_{\perp} \leq \lambda_{\perp}/a_0 \lambda_{\parallel}$ provide the dominating contribution to the thermal noise.

At very high frequencies, $\omega_{\lambda} \ll \omega \ll \omega_d$, tilt modes with wave vectors $q_{\perp} \leq (2\pi \eta \omega / \alpha \phi_0 B)^{1/2}$ are engaged in voltage-noise generation and the power-spectrum shape is determined by the short-wave Josephson part of the tilt modulus. Thus for very high frequencies we have

$$S_v(\omega) = \frac{(\phi_0 B)^{1/2} T L}{8 W c^2 \eta^{1/2}} (2\pi \omega / \alpha)^{1/2}. \quad (51)$$

At ultrahigh frequencies, above the highest characteristic frequency ω_d , one can write $\eta_p \omega \gg (\phi_0 d/B) C_{44} \bar{q}_{\perp}^2$ for all q_{\perp} and the resulting power spectrum becomes white again:

$$S_v(\omega) = S_{v2} = \frac{\phi_0 B L T}{4c^2 W \eta d}. \quad (52)$$

Let us observe that the magnitude of white spectral density at ultrahigh frequencies, $\omega \gg \omega_d$, is $D/2d$ times larger than the white spectrum density at low frequencies, $\omega \ll \omega_D$; see Eq. (42). The value of the ratio D/d is set by the number of layers N_L in the strip or, in other words, by the number of pancakes in a single vortex stack. This result is physically transparent. Indeed, at low frequencies only one degree of freedom per one flux line contributes to the thermally activated noise power spectrum, whereas, at high frequencies, all degrees of freedom are engaged in the voltage-noise generation causing a significant, approximately N_L times increase in the power-spectrum magnitude.

C. Fluctuations of flexible pancake strings: High magnetic fields

At strong magnetic fields exceeding the crossover threshold field only magnetic interaction between the lay-

ers is significant, i.e., the first term in Eq. (11) prevails at all \mathbf{q}_\perp . In order to calculate spectrum (44) we divide the integration range $(0, \pi/d)$ into two subintervals; from 0 to $1/\lambda_\parallel$ and from $1/\lambda_\parallel$ to π/d . The kernel in the latter interval can be approximated by a constant. We have used for the constant $(\phi_0 d/B)C_{44}\bar{q}_\perp^2 \approx \eta_p \omega_\lambda$, and obtained

$$\int_{1/\lambda_\parallel}^{\pi/d} \frac{\omega^2 d \mathbf{q}_\perp}{[(\phi_0 d/B)C_{44}]^2 \bar{q}_\perp^4 + \eta_p^2 \omega^2} \approx \frac{\pi}{d \eta_p^2} \frac{\omega^2}{\omega^2 + \omega_\lambda^2}. \quad (53)$$

The value of the integral calculated in the limits $(0, 1/\lambda_\parallel)$ is small in comparison with Eq. (53) for all frequencies lying above the characteristic frequency ω_λ . On the other hand, for the low-frequency range, $\omega_D \ll \omega \ll \omega_\lambda$, this subintegral can be calculated as follows:

$$\begin{aligned} \int_0^{1/\lambda_\parallel} \frac{\omega^2 d \mathbf{q}_\perp}{[(\phi_0 d/B)C_{44}]^2 \bar{q}_\perp^4 + \eta_p^2 \omega^2} \\ \approx \int_0^\infty \frac{\omega^2 d \mathbf{q}_\perp}{(\phi_0 B d/4\pi)^2 \bar{q}_\perp^4 + \eta_p^2 \omega^2} = \frac{\pi^{3/2} \omega^{1/2}}{(2\phi_0 B)^{1/2} \eta_p^{3/2} d^2}. \end{aligned} \quad (54)$$

Thus we can write for the power spectrum for frequencies $\omega \gg \omega_D$

$$S_v(\omega) = \frac{\phi_0 B L T}{4\eta c^2 W} \left[\left(\frac{\pi \eta \omega}{2\phi_0 B} \right)^{1/2} + \frac{\omega^2/d}{\omega^2 + \omega_\lambda^2} \right]. \quad (55)$$

Clearly, as in the previously discussed case, there is a change of the spectrum functional dependence at a frequency of the order of

$$\omega_c \sim \frac{\phi_0 d^{2/3}}{8\pi \eta \lambda_\parallel^{8/3}} B. \quad (56)$$

Note that the characteristic frequency at which the exponent of the power spectrum changes from $\frac{1}{2}$ to 2 is different from that determined for low magnetic fields; see Eq. (50). In particular, the magnetic field dependence of the characteristic frequency is stronger at fields above the crossover field.

Since the Josephson coupling term is negligible at strong magnetic fields above the crossover, there is no subsequent $\omega^{1/2}$ -like magnitude increase and the voltage-fluctuation spectrum becomes white already at $\omega \sim \omega_\lambda$. In Fig. 2 we schematically summarize the discussed behavior of thermal-voltage power spectra for magnetic fields below and above the crossover field.

The results presented above are valid for systems with moderate anisotropy, $\lambda_1 d \ll \lambda_\parallel^2$. For strongly anisotropic systems, where $\lambda_1 d \gg \lambda_\parallel^2$, the situation is much simpler and the power spectrum due to fluctuations of flexible vortices at frequencies $\omega \gg \omega_D$ is given by Eq. (51) for all magnetic fields.

D. Fluctuations of flexible pancakes strings in layered high- T_c superconductors

In high-temperature superconducting (HTSC) materials the role of superconducting layers is played by CuO_2 layers. In real compounds with a pronounced layered quality, such as, e.g., (2212) Bi-Sr-Ca-Cu-O, there is more than one layer per unit cell. The coupling between intra-unit cell layers is much stronger than the interunit cell coupling. Therefore we consider the real layered HTSC material as being composed of layers of strongly coupled intracell sublayers. Consequently, a flexible vortex stack consists of Josephson-coupled flexible pieces of 3D vortices located within the intracell layers. Tilt-mode excitations of these pieces contribute to the power spectra of voltage noise at very high frequencies. In the following we consider the power spectrum due to tilt fluctuations of flexible vortex segments in intracell layers. In principle, one should calculate first the elastic modulus of the entire vortex system including intracell-vortex short-wave

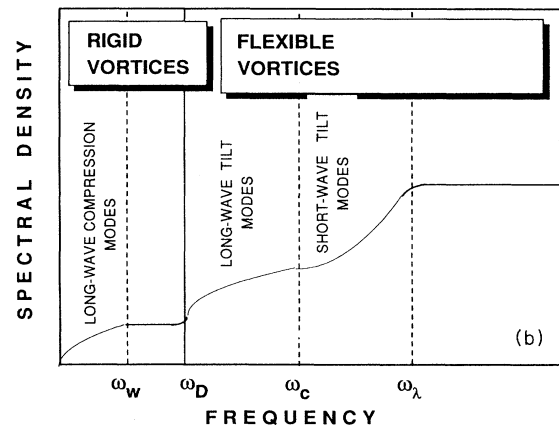
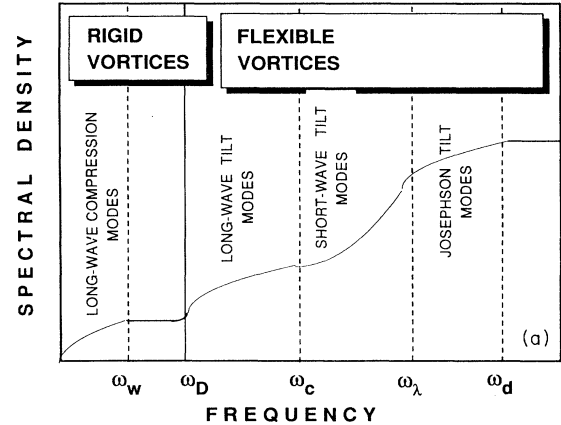


FIG. 2. Schematic behavior of thermal-voltage-noise power spectrum: (a) low magnetic fields $B < B_{th}$ and (b) strong magnetic fields $B > B_{th}$.

modes. However, as will be shown below, the characteristic frequencies of onset of these modes are well above all remaining frequencies of the problem. Therefore we are allowed to treat these fluctuations as independent additive contributions to the power spectrum. Employing the general Eq. (38) which is valid for continuous vortices we obtain for the power spectrum of the discussed intracell contributions

$$S_v(\omega) = \frac{\phi_0 B L T \eta}{8\pi c^2 W} \int_{1/d_1}^{1/\xi_1} \frac{\omega^2 d \mathbf{q}_\perp}{[(\phi_0/B)C_{44}]^2 \mathbf{q}_\perp^4 + \eta^2 \omega^2}, \quad (57)$$

where the modulus

$$C_{44} = \frac{B^2}{4\pi(1+\Lambda^2 \mathbf{q}^2)} + \frac{\phi_0 B \ln \kappa}{4\pi \Lambda^2}, \quad (58)$$

d_1 is the distance between intracell superconducting layers, Λ is the London penetration length in these layers, $\mathbf{q} = (\mathbf{q}_\perp, \mathbf{q}_\parallel)$, and $\kappa = \Lambda/\xi$. In this approach which accounts for the internal structure of unit cells, the previously introduced quantity d denotes now the separation between the cells. The evident condition $B \ll \phi_0/d_1^2$ enables us to neglect the first term in Eq. (58). As a result, integral (57) gets an extremely simple form which can be easily evaluated in different frequency ranges:

(1) $\omega \ll \omega_{c1} \ll \omega_{c2}$.

$$S_v(\omega) = \frac{\phi_0 B L T}{8\pi c^2 \eta W d_1} \left[\frac{\omega}{\omega_{c1}} \right]^2, \quad (59)$$

where

$$\omega_{c1} = \frac{\phi_0^2 \ln \kappa}{4\pi \eta \Lambda^2 d_1^2} \quad \text{and} \quad \omega_{c2} = \frac{\phi_0^2 \ln \kappa}{4\pi \eta \Lambda^2 \xi_1^2}.$$

(2) $\omega_{c1} \ll \omega \ll \omega_{c2}$.

$$S_v(\omega) = \frac{\phi_0 B L T}{32c^2 \eta W d_1} \left[\frac{\omega}{2\omega_{c1}} \right]^{1/2}. \quad (60)$$

(3) $\omega_{c2} \ll \omega$.

$$S_v(\omega) = S_{v3} = \frac{\phi_0 B L T}{8\pi c^2 \eta W \xi_1}. \quad (61)$$

It should be noted here that the spectral density of the intracell vortex fluctuations leads to the same functional behavior of the power spectrum as those due to lower-frequency modes. We conclude that intracell vortices cause the appearance of an additional spectrum increase at ultrahigh frequencies $\omega \gg \omega_{c1} \gg \omega_d$. The magnitude of the very high frequency plateau S_{v3} exceeds drastically the magnitude of plateaus resulting from saturation of lower-frequency modes. Indeed, the ratio S_{v3}/S_{v2} scales as $d/\xi_1 \gg 1$.

IV. CONCLUSIONS

In conclusion, we have shown that allowing for flexibility of vortex strings, i.e., taking into account the excitation of tilt modes of vortices, leads to qualitatively new effects that manifest themselves in thermal-voltage-noise

power spectra at high frequencies above the characteristic frequency set by the strip thickness. Below this frequency, excitation of rigid-vortex long-wave modes causes initial increase of the power spectrum and its saturation at a characteristic frequency depending on the dimensions of the voltage measuring circuit. This regime of thermal fluctuations has been already discussed by Li and Clem.¹

The flexibility of vortices causes additional increases of the power spectra at frequencies corresponding to the onsets of tilt modes. The tilt fluctuation modes should be most pronounced in layered superconducting systems with a moderate anisotropy where vortices consist of loosely coupled pancake stacks. For such systems, at low magnetic fields, we predict three subsequent increases of thermal-voltage-power spectra. The increases follow $\omega^{1/2}$, ω^2 , and again $\omega^{1/2}$ behavior. The first high-frequency $\omega^{1/2}$ -like region corresponds to the long-wave tilt-mode fluctuations. With increasing frequency, tilt modes with shorter wavelengths start to contribute to the voltage noise and the spectrum functional dependence changes into ω^2 -like behavior, at frequencies above the magnetic-field-dependent characteristic frequency. The highest-frequency increase in voltage power spectra is associated with excitations of short-wave tilt modes controlled by the Josephson coupling energy between the layers. Finally, when all degrees of freedom of the vortex system become thermoactivated the power spectrum becomes white again. The high-frequency white noise magnitude is $D/2d$ times higher than the white spectrum level in the Li and Clem regime of thermal fluctuations of rigid vortices.

The overall picture is magnetic field dependent. There is a characteristic threshold field B_{th} , corresponding to the well-known 2D/3D lattice melting crossover field [5], at which the pronounced change in spectral behavior takes place. At magnetic fields above the crossover field the functional dependence of the characteristic frequency separating long-wave and short-wave tilt modes, i.e., the first $\omega^{1/2}$ -like and subsequent ω^2 regions, changes from $\omega_c \sim B^{2/3}$ into a stronger $\omega_c \sim B$ dependence; see Eqs. (50) and (56). Moreover, the second $\omega^{1/2}$ -like magnitude increase vanishes and the power spectrum saturates after the ω^2 region. These features are due to the smallness of the Josephson coupling with respect to magnetic interactions between vortices at high magnetic fields.

The voltage-noise power spectrum of a continuous anisotropic superconductor containing flexible vortices can be derived straightforwardly from the equations obtained in Secs. III B and III C for layered superconductors with moderate anisotropy by substituting the interlayer spacing d with coherence length ξ_1 . The results will be valid at all magnetic fields $B_{c1} \ll B \ll B_{c2}$. Observe that in the continuous superconductor case the threshold field given by Eq. (45) is

$$B_{th} \sim \frac{\phi_0^2 \lambda_\parallel^2}{(4\pi \lambda_\perp \xi_1)^2} \sim \frac{\phi_0^2}{(4\pi \xi_\parallel)^2} \sim B_{c2} \quad (62)$$

and corresponds directly to the second critical field, as

follows from the definitions of coherence length and penetration depth. Therefore the predicted crossover in spectral behavior at the crossover magnetic field turns out to exist *exclusively* in layered superconductors.

In high- T_c materials with pronounced layered character we predict an additional increase in power spectra at ultrahigh frequencies due to intracell fluctuations of vortices. However, experimental observations of the predicted effects of vortex flexibility in, e.g., Tl-based compounds, would require use of microwave techniques. The characteristic lengths of these superconductors are of the order $\lambda_{\parallel} = 2 \times 10^{-5}$ cm, $d = 2 \times 10^{-7}$ cm, $\lambda_1/\lambda_{\parallel} \approx 30$, $\xi_{\perp} \approx 10^{-8}$ cm, and $d_1 \approx 5 \times 10^{-8}$ cm.¹⁴ According to NMR data on relaxation rates in Tl₂Ba₂CuO₆, the vortex viscosity per unit length is of the range $\eta \approx 10^{-7} - 10^{-6}$ g/cm s.⁴ The crossover field for Tl-based compounds was estimated to be $B_{\text{th}} \sim 1$ T.⁵ For a strip with sizes $L \approx 1$ cm, $W \approx 10^{-2}$ cm, and $D \approx 10^{-4}$ cm we obtain, in the

field range from 0.1 up to 10 T, the following values for the characteristic frequencies: $\omega_w/2\pi \sim B(10^6 - 10^5)$ Hz, $\omega_D/2\pi \sim B(10^{10} - 10^9)$ Hz, $\omega_c/2\pi \sim B^{2/3}(10^{11} - 10^{10})$ Hz, for $B < B_{\text{th}}$, and $\omega_c/2\pi \sim B(10^{11} - 10^{10})$ Hz for $B > B_{\text{th}}$, $\omega_{\lambda}/2\pi \sim B(10^{12} - 10^{11})$ Hz, $\omega_d/2\pi \sim (10^{12} - 10^{11})$ Hz, $\omega_{c1}/2\pi \sim (10^{13} - 10^{12})$ Hz, and $\omega_{c2}/2\pi \sim (10^{14} - 10^{13})$ Hz where B is measured in T. The magnitudes of the spectral density of thermal voltages, for $T \sim 30$ K and $B \sim 10$ T, at high- and very-high-frequency plateaus, are of the order $S_{v2} \sim 10^{-17} - 10^{-16}$ V²/Hz and $S_{v3} \sim 10^{-16} - 10^{-15}$ V²/Hz, respectively.

ACKNOWLEDGMENTS

We would like to thank the Ministry of Science and Technology, Israel Academy of Sciences, and German-Israel and Rashi Foundations for their support.

¹P. S. Li and J. R. Clem, Phys. Rev. B **23**, 2209 (1981).

²J. R. Clem, Phys. Rep. **75**, 1 (1981).

³T. Hocquet, P. Mathieu, and Y. Simon, Phys. Rev. B **46**, 1061 (1992).

⁴L. N. Bulaevskii, N. N. Kolesnikov, I. F. Schegolev, and O. M. Vyaselev, Phys. Rev. Lett. **71**, 1891 (1993).

⁵M. V. Feigelman, V. B. Geshkenbein, and A. I. Larkin, Physica C **167**, 177 (1990).

⁶L. I. Glazman and A. E. Koshelev, Phys. Rev. B **43**, 2835 (1991).

⁷L. L. Daemen, L. N. Bulaevskii, M. P. Maley, and J. Y. Coulter, Phys. Rev. B **47**, 11 291 (1993).

⁸W. E. Lawrence and S. Doniach, in *Proceedings of 12th International Conference on Low Temperature Physics, Kyoto, 1970*, edited by E. Kanda (Keigaku, Tokyo, 1970).

⁹E. H. Brandt, J. Low Temp. Phys. **26**, 709 (1977); **28**, 291 (1977).

¹⁰A. Houghton, R. A. Pelkovits, and A. Sudbo, Phys. Rev. B **40**, 6763 (1989).

¹¹D. J. van Ooijen and G. J. van Garp, Phys. Lett. **17**, 230 (1965); Philips Res. Rep. **20**, 505 (1966).

¹²L. N. Bulaevskii and M. P. Maley, Phys. Rev. Lett. **71**, 3541 (1993).

¹³V. D. Ashkenazy, G. Jung, I. B. Khalfin, and B. Ya. Shapiro, Physica C **224**, 377 (1994).

¹⁴D. E. Farrell, S. Bohnham, J. Foster, Y. Chang, P. Z. Jiang, K. G. Vandervoort, D. L. Lam, and V. G. Kogan, Phys. Rev. Lett. **63**, 782 (1989); K. E. Gray, R. T. Kampwirth, and D. E. Farrell, Phys. Rev. B **41**, 819 (1990).